Materials Advances

ROYAL SOCIETY OF CHEMISTRY

PAPER

View Article Online
View Journal | View Issue

Cite this: *Mater. Adv.*, 2026, 7, 3268

3D DLP printed mechanochromic materials for visual signaling

Finn Kröger, [ab] Christoph A. Spiegel [ab] and Eva Blasco *[ab]

Mechanophores offer a unique approach to visualize stress *via* color change as a response to mechanical force. Their integration into polymeric materials has opened new pathways for real-time damage sensing and failure detection. When combined with additive manufacturing technologies, particularly high-resolution light-based 3D printing, mechanophore-based systems present great potential for developing functional materials with embedded signaling capabilities. In this work, we present new materials for digital light processing including spiropyran moieties as mechanophores. In particular, a spiropyran equipped with two photopolymerizable groups is synthesized and included into two printable formulations based on the monomers methyl acrylate and acrylic acid. The careful selection of the photoinitiator and crosslinker has enabled the 3D printing of complex 3D geometries, which visually respond to compression and tensile stress. The mechanochromic effect is demonstrated by the compression of a tube and a pad, which respond with a color change towards purple. Irradiation with visible light leads to a recovery in color and towards the shape before compression. Employing 3D printed "dog bones" as specimens, mechanochromic behavior is successfully demonstrated in response to tensile stress, initiating a similar change in color. Overall, the presented system shows great promise for creation of functional, high-resolution sensing 4D materials.

Received 2nd December 2025,
Accepted 16th February 2026

DOI: 10.1039/d5ma01401h

rsc.li/materials-advances

1. Introduction

Polymer materials are widely used across numerous applications and are frequently exposed to substantial mechanical stress, which can result in creep, fatigue, or fractures of individual polymer chains.[1–3] To detect such damage at an early stage, mechanophores are particularly useful as they exhibit a distinct and easily perceptible color change in response to mechanical force.[4,5] Acting as "warning systems", the mechanophores can prevent catastrophic material failures before macroscopic damage occurs. Commonly investigated mechanophores include spiropyran-,[6–8] difluorenylsuccinonitrile-,[9,10] triarylmethane-,[11,12] diarylbibenzofuranone-,[13–15] and diarylbibenzothiophenonyl-derivatives.[13,16] Among these, particular attention has been given to spiropyran (Sp) derivatives, which can be activated by mechanical force,[6–8] UV-light,[17,18] and ultrasonic waves.[19,20] Upon activation, Sp undergoes isomerization from its colorless, closed-ring form to a colored, zwitterionic open-ring structure known as merocyanine (Mc).[21] Typically, the polymer matrices consist of long, linear chains with minimal or no crosslinking, which is crucial for enabling mechanoresponsive behavior.[22,23] Most of the reported systems that implement a mechanophore in the polymer matrix are processed by molding.[6,17,24–26] For instance, in a pioneering study by Davis *et al.*,[7] Sp moieties were covalently incorporated into polymethacrylate (PMA) and used as crosslinkers. The mechanoresponse of molded "dog bone" specimens and crosslinked beads prepared from these Sp-containing materials were investigated under tensile loading and compression, respectively. Importantly, the authors demonstrated that the mechanophoric functionality is solely integrated into the cured material when the Sp, functionalized with a polymerizable moiety on both sides of the sp^3-hybridized spiro carbon atom, is covalently incorporated into the polymeric network *via* both respective sites. It was further shown that integration of monofunctional or difunctional Sp, with one or two polymerizable groups on one side of the sp^3-hybridized spiro carbon atom, results in the absence of a mechanophoric response in the polymeric network. This approach represents an important advancement in visualizing mechanical activation; however, the reliance on molds constrains the ability to shape the material into more complex and application-specific geometries.

Three-dimensional (3D) printing, also known under the term additive manufacturing (AM), enables the faster and more flexible production of complex structures from digital 3D designs. In the last years, initial progress has been made towards the integration of mechanophores into AM-compatible

[a] *Institute for Molecular Systems Engineering and Advanced Materials, Heidelberg University, Im Neuenheimer Feld 225, 69120 Heidelberg, Germany. E-mail: eva.blasco@uni-heidelberg.de*
[b] *Institute of Organic Chemistry, Heidelberg University, Im Neuenheimer Feld 270, 69120 Heidelberg, Germany*

formulations.[27] For example, Boydston and coworkers employed Sp-containing poly(ε-caprolactone) (PCL) polymers to fabricate single and multi-materials specimens *via* filament extrusion.[24] Using AM's unique capabilities, they demonstrated a simple force sensor that allows peak load assessment through straightforward visual detection of mechanochromism. More recently, the same group also reported the manufacturing of mechanochromic materials based on Sp-containing PCL polymers using powder material extrusion.[28] In another interesting work, Nelson and coworkers demonstrated the direct-ink writing of mechanochromic ionic liquid gels by incorporating dimethacrylated Sp as crosslinker.[29]

In particular, light-based technologies, such as digital light processing (DLP), are very attractive for the fast fabrication of complex 3D structures with an outstanding precision and smooth surface finish.[30,31] Very recently Loos group reported an interesting work using different Sp derivatives in formulations for DLP printing.[32] They integrated dynamic disulfides and β-hydroxy esters into the printable material, enhancing it with Sp as a non-covalently bound additive, enabling tunable photochromic and thermochromic properties. Despite this example, the implementation of mechanoresponsive functionality in DLP systems remains largely unexplored, even though it has large potential to open promising avenues in engineering of smart, customized sensors.

Herein, we present new formulations including a photopolymerizable mechanophore that enables the precise fabrication of complex mechanochromic 3D structures *via* DLP printing, which are capable of reporting a color change in response to either stretching or compression (Fig. 1). To this aim, spiropyran (Sp) is selected as a suitable mechanophore and is equipped with two acrylate groups (Sp-dA) on either side of the sp^3 hybridized carbon atom, enabling its efficient incorporation into a (meth)acrylate-based network. Next, formulations including Sp-dA are developed and optimized to achieve good printing performance as well as a reliable mechanochromic response. In this context, the choice of appropriate monomers – such as methyl acrylate and acrylic acid – is crucial. Additionally, the crosslinker concentration is systematically evaluated. Optimized formulations are employed for fabrication of complex 3D structures like ''benchies''. Furthermore, the response towards mechanical stress, more precise compression and stretching, as well as their recovery in color and shape are investigated. These advancements significantly enhance 4D printable materials, enabling reliable mechanochromic visual signaling.

2. Results and discussion

2.1. Mechanophore-containing formulations for DLP printing

To enable the 3D fabrication of mechanochromic materials *via* digital light processing (DLP), suitable photopolymer formulations incorporating mechanophores were developed. SP was identified as ideal candidate for this purpose owing to its mechanochromic behavior and straightforward functionalization. To ensure the efficient incorporation of the mechanophore species into the polymer network during DLP 3D printing, we target the synthesis of a Sp derivative equipped with two acrylate groups. Acrylates were chosen over methacrylates as photopolymerizable moieties due to their higher reactivity.[7,17,33,34] To this aim, a literature known Sp-diol was synthesized and further functionalized by introducing acrylate moieties *via* esterification with acryloyl chloride to obtain Sp-diacrylate (Sp-dA). The successful synthesis of Sp-dA was confirmed *via* ^{1}H and ^{13}C NMR spectroscopy (see SI, Fig. S5 and S6).

Next, the synthesized photocrosslinkable mechanophore Sp-dA was introduced into a formulation suitable for DLP printing. Along with the mechanophore which also acts as a crosslinker in this case, the selection of the photoinitiator, the monofunctional monomers acting as chain builders of the polymer matrix, and other additives were key to obtaining a printable formulation but also to ensure a visual response to mechanical forces in particular compression and stretching.

Standard photoinitiators for DLP 3D printing such as phenyl-bis(2,4,6-trimethylbenzoyl)phosphinoxid (BAPO) are efficient in the 365 to 405 nm wavelength regime, which most DLP printers use. However, the mechanophore Sp-dA exhibits significant absorption in this region (see SI, Fig. S7) and due to relatively high concentration in the formulation (1.0 wt%), this strong absorption significantly hinders the photopolymerization, rendering the 405 nm wavelength LED unsuitable for 3D DLP printing.[35] Moreover, irradiation with 405 nm wavelength light induces the isomerization to merocyanine (Mc), which would require post-processing to switch the mechanophore back to the Sp form. Thus, 460 nm was selected as printing wavelength since no absorption at longer wavelength than 420 nm was detected for Sp-dA and Ivocerin was chosen as a photoinitiator enabling efficient printing at this longer wavelength.[36,37] Also, no isomerization of the Sp occurs at this wavelength.

Targeting efficient mechanochromic behavior for later printed materials, the ink composition was designed to achieve printed networks which exhibit a low degree of crosslinking. It is reported that polymer networks with a low crosslinking degree, result in an increased chain mobility having a favorable impact on mechanochromic characteristics.[6,7,38,39] Initial formulations were composed mainly of methyl methacrylate (MeA) as chain builder and low amounts of Sp-dA as a crosslinker. However, it was not sufficient to create a stable network. Hence, additional crosslinker, *i.e.*, ethylene glycol dimethacrylate (EGDMA), was added to the formulation to increase the crosslinking density and improve printability. It was found that an EGDMA content of 11.2 wt% allowed efficient 3D DLP printing. Furthermore, to avoid precipitation of the mechanophore during printing, small amounts of solvent, in this case 1,4-dioxane (dioxane) were added. Thus, the optimized formulation consisted of MeA (84.9 wt%), EGDMA (11.2 wt%), Ivocerin (1.0 wt%), Sp-dA (1.0 wt%), and dioxane (1.9 wt%) (Fig. 2a).

Once the formulation was established, curing tests were performed to evaluate optimal 3D printing conditions

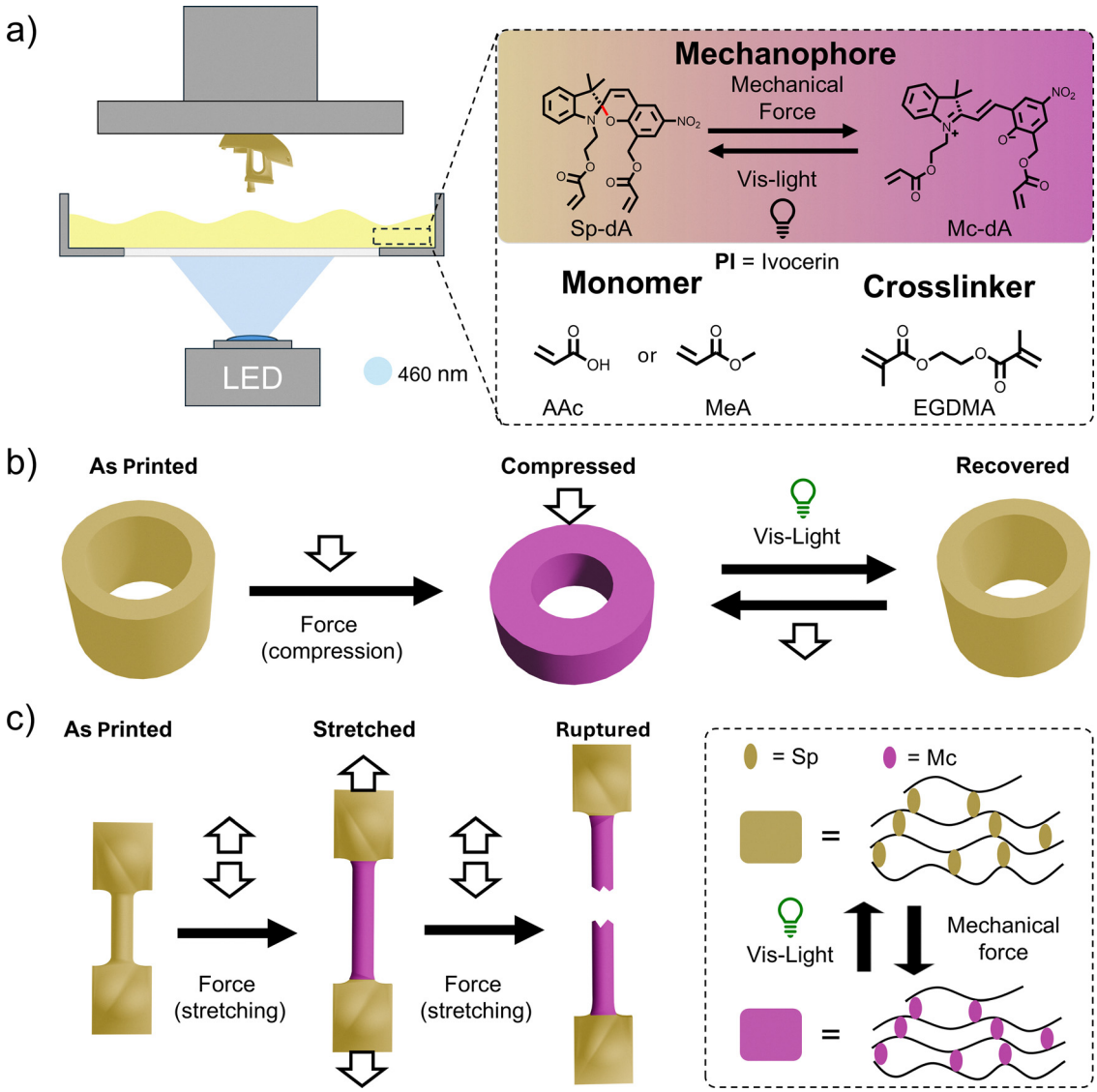

Fig. 1 (a) Left: Scheme of a DLP printer. Right: Printable formulation including: acrylated mechanophore Sp-dA, acrylic acid (AAc) and methyl acrylate (MeA) as monomers, ethylene glycol dimethacrylate (EGDMA) as additional crosslinker, and Ivocerin as photoinitiator. (b) Schematic representation of the compression experiment: a 3D printed tube (as printed) is exposed to mechanical force (compression). As a result, the mechanophore is activated and a color change occurs. The initial shape and color can be recovered by irradiation with visible light. (c) Schematic representation of the tensile stress experiments: a 3D printed "dog bone" specimen (as printed) is stretched, resulting in a color change in the thinner area of the specimen where the stress is applied, until rupture.

(see 4.2 Methods). In particular, Jacobs working curves were generated by plotting the experimentally determined curing depths against the corresponding exposure energies in a semi-logarithmic plot (Fig. 2b). The interception with the *x*-axis describes the energy necessary to reach the gel point of the formulation and is termed critical energy (E_c).[40] The E_c was determined to be 315 mJ cm^{-2} at the curing wavelength of 460 nm. On the basis of the Jacobs working curve analysis optimal printability was achieved by employing a curing intensity of 14 mW cm^{-2} and an irradiation time of 32 s, accessing a curing layer thickness of 100 µm. Applying these parameters, a lateral printing resolution of 75 µm and a minimal linewidth of 79 µm were obtained (see SI, Fig. S8). The small minimal feature size and good resolution highlight the potential to DLP print 3D structures with outstanding precision. This was further validated by the successful fabrication of complex geometries, including the standard benchmarking boat structure "benchy" (Fig. 2c). FTIR measurements of the formulation and the printed structure allowed the calculation of a double bond conversion, which was determined at 96% (see SI, Fig. S11).

To confirm the incorporation of Sp into the 3D-printed material, its photoresponse and more specifically the reversible isomerization to the colored Mc form, was investigated, hereby demonstrating its potential as a self-reporting material. First, absorption measurements of films prepared by photocuring the established formulation were performed. In its initial cured state, with the mechanophore predominantly in the Sp form,

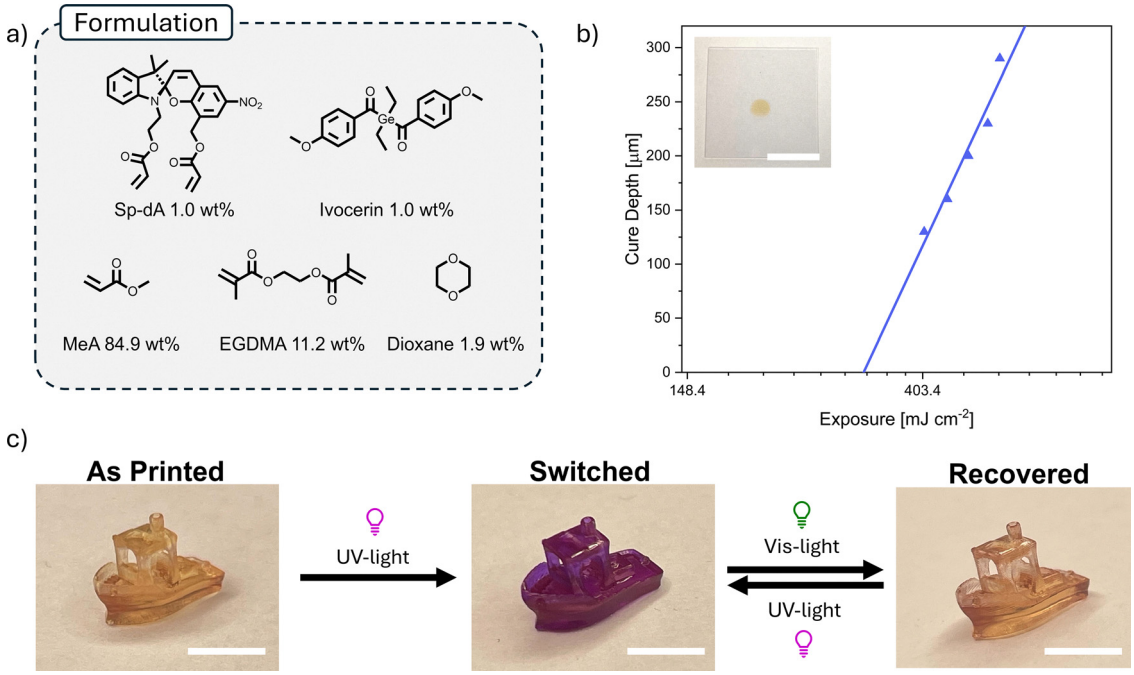

Fig. 2 (a) Optimized formulation consisting of the mechanophore Sp-dA, Ivocerin as a photoinitiator, MeA as monomer, EGDMA as a crosslinker and dioxane as solvent. (b) The Jacobs working curve of the optimized formulation, including one exemplary cured circular spot, are shown. (c) 3D printed benchmarking structure "benchy (as printed), after UV-light irradiation (switched) and after visible light irradiation (recovered) showcasing the reversible activation of the mechanophore (Scalebars = 5 mm).

the material exhibits a pale-yellow color, characterized by its main absorption in the UV region and negligible absorption above 460 nm (see SI, Fig. S9). After 3 minutes of UV irradiation, an additional absorption peak with a maximum at 585 nm - corresponding to the Mc form - was observed, consistent with the behavior of the free mechanophore Sp-dA in solution (see SI, Fig. S7). In addition, the same irradiation experiment was carried out using a 3D printed benchmarking structure called "benchy" (Fig. 2c). As expected, the color switched from pale yellow to purple, indicating that the Sp is incorporated into the bulk structure and can be efficiently activated. Moreover, irradiation with visible light restored the original pale-yellow color by switching the mechanophore from the Mc state back to Sp. Such reversible switching between Sp and Mc in the 3D structure was repeatable at least five times without any detectable degradation. Subsequently, dynamic mechanical analysis (DMA) measurements were performed to gain more insight into thermal and thermomechanical properties of the developed 3D printed material. For this purpose, $15 \times 3 \times 1$ mm^3 bars were printed, and employed for DMA measurements in a temperature range from -70 to 160 °C (see SI, Fig. S10). A storage modulus of 890 MPa was evaluated at 20 °C as well as a glass transition at 53 °C by analysis of the corresponding tan(δ) curve, which also showed a small shoulder at 18 °C, suggesting that the system exhibits multiple phases.

2.2. Mechanochromic response to compression

As a next step, the response of the material to compressive forces was evaluated. For this purpose, a pad ($12 \times 12 \times 1$ mm^3) and a tube (outer diameter 10 mm, wall thickness 2 mm, and height 4.5 mm) were 3D printed using the optimized formulation and subjected to mechanical stress in the form of compression. First, the pad was exposed to pressure with a circular stamp resulting in a purple ring that matched the compressed area, confirming the activation of the Mc form (Fig. 3a). Notably, it was possible to "delete" the generated pattern by reverting the Mc form back to the Sp *via* irradiation with visible light, demonstrating the reversible nature of the incorporated mechanophore. It is worth noting that the entire sample got a slightly darker color. This compression–recovery cycle was repeatable over multiple iterations.

Second, the influence of mechanical stress in the form of compression on the bulk material was also tested (Fig. 3b). To this end, the 3D printed tube was subjected to compressive mechanical forces using a vise with a caliper to measure the compressed distance. The printed tube was initially 4.5 mm high and pale-yellow, upon compression to a height of 2.8 mm, it turned purple. After releasing the pressure, the tube partially expanded to a height of 3.2 mm, but the mechanophore remained in the Mc form, causing the tube to retain its purple color (Fig. 3b). Subsequent irradiation with visible light for 10 min restored both the original yellowish color and the tube's height of 4.5 mm. The compression and recovery cycles were performed five times and no difference in the recovery was detected proving the good performance of the mechanochromic material in bulk.

2.3. Mechanochromic response to tensile forces

After successfully proving the mechanochromic response by compression, our next goal was to develop a printable

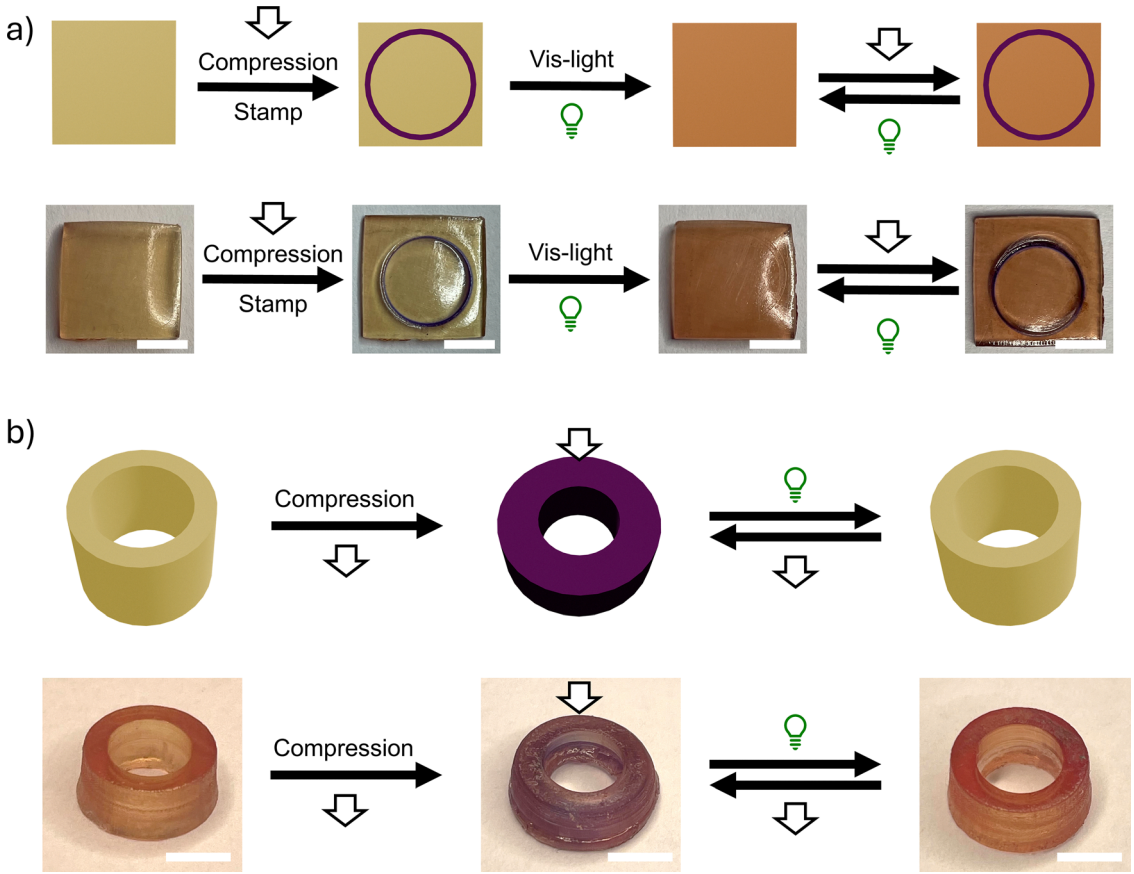

Fig. 3 (a) Schematic representation (top) and photographs of the 3D printed pad (bottom) as printed (yellow) and after compression with a stamp in a circular shape. A purple-colored ring is visible in the compressed areas. After visible light irradiation, no indentation is visible, and the purple color is erased. Multiple stamps and visible light irradiation cycles can be performed, demonstrating the reversibility of the process. (b) A schematic representation (top) and photographs of the 3D printed tube (bottom) as printed (yellow) and after compression (purple) are shown. Irradiation with visible light restored both the color and shape. Multiple compression and visible light irradiation cycles can be conducted, showing the reversibility of the process (Scalebars = 5 mm).

material that could visually signal the presence of tensile stress. In the previous formulation, significant amounts of crosslinker were necessary to obtain good printability, resulting in a material elasticity insufficient to detect the stretching before the material ruptures (see SI, Fig. S12). Thus, the development of new formulations with a reduced amount of crosslinker were targeted without compromising the printability. As monomers acrylic acid (AAc) and *N*,*N*-dimethyl acrylamide (DMAA) were taken into consideration. As crosslinkers, 1.7 wt% of Sp-dA and a lower concentration of EGDMA (2.0 wt%) were used. Initial tests showed good printability, but the formulation containing DMAA did not show a visual response to tensile stress. Thus, the AcA-based formulation containing AcA (95.2 wt%), EGDMA (2.0 wt%), Ivocerin (1.1 wt%), and Sp-dA (1.7 wt%) was selected for further studies.

To gain insights into the curing properties and to determine optimal irradiation conditions for the established formulation, a Jacobs working curve was plotted on the basis of the measured curing depths and respective energies, leading to an E_c of 115 mJ cm^{-2} (see SI, Fig. S13). Irradiation times of 15 s applying a 460 nm wavelength LED at an intensity of 14 mW cm^{-2} were found to be optimal for DLP printing. As with the previous formulation, a good resolution of 90 μm and a minimal feature sizes of 94 μm were determined (see SI, Fig. S8). To demonstrate the printing performance of this formulation and the activation of the printed material further, a ''benchy'' was 3D printed and irradiated with UV-light. The color switched from yellow to red (Fig. 4a) and could be reverted by irradiation with visible light (see SI, Fig. S14). To confirm this, absorption measurements were carried out on cured films using this formulation. In its initial state, absorption in the UV r egion was measured, along with negligible absorption above 460 nm. After irradiation with UV-light, an additional absorption peak with a maximum at 520 nm corresponding to the Mc form was observed (see SI, Fig. S9). Compared to the previous MeA-based material, a 65 nm red-shift was monitored. This can be explained by the negative solvatochromic effect, which was also detected in solution (see SI, Fig. S7). The printed polymer network consists mostly of polyacrylic acid, which is significantly more polar than the previous MeA-based matrix.

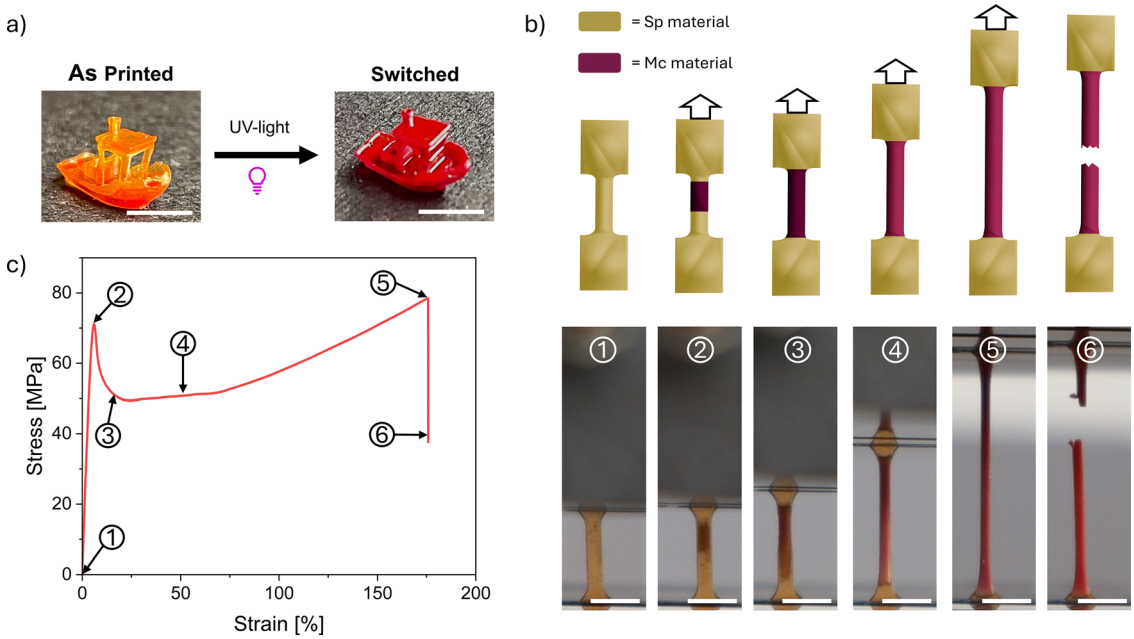

Fig. 4 (a) A 3D DLP printed "benchy" is shown as printed and after being irradiated with UV-light. (b) A schematic representation (top) of the stretching of the "dog bone" and a 3D printed "dog bone" (bottom) at different strain levels (0 to 175%) and the ruptured specimen are depicted (see SI for video). (c) The stress strain curve of the tensile test is shown (Scalebars = 5 mm).

Initial mechanical analysis was performed by DMA characterization of 3D printed bars ($15 \times 3 \times 1$ mm^3). The obtained tan(δ) curve shows a main peak corresponding to a glass transition temperature at 46 °C. In addition, the thermogram also revealed a shoulder at 78 °C, indicating the presence of multiple phases within the polymeric network. The storage modulus at 20 °C was determined at 1.2 GPa (see SI, Fig. S10).

To investigate the mechanoresponse, "dog bones" specimens were 3D printed using the AcA-based formulation and employed for tensile tests. Fig. 4b depicts the sample at different amounts of strain. First, the specimen was fixed between the clamps of the tensile test device. In this state the material experienced no stress (point 1, 0% strain) and remained yellow, indicating that the mechanophore was in its Sp state. To apply strain to the sample, the clamps were moved apart at a speed of 4 mm per minute. The yield point (point 2) was reached at a strain of 6% with a stress of 70 MPa, here also the initial color change was observed, indicating that the Sp was switched to the colorful Mc. During the necking phase (point 3), which happened at a strain of 22%, the stress reduced to 50 MPa and now a distinct color change from yellow to dark red was visible throughout the entire sample. This phase is followed by a plastic deformation (point 4) until a strain of 70%, which was accompanied by no significant color change of the sample. Afterwards the strain hardening regime was detected, where the sample maintained constant color and reached its ultimate strength. Overall, the sample was able to withstand stresses up to 79 MPa with strains up to 175% (point 5) before it ruptured (Fig. 4b and c; see Video in the SI).

3. Conclusion

In summary, we successfully synthesized a photocrosslinkable mechanophore and incorporated it into a formulation for DLP printing. Two different formulations based on methyl acrylate (MeA) and acrylic acid (AcA) were optimized to yield not only robust and reliable 3D printing performance but also enable the visual signaling of mechanical force. In both cases, complex 3D geometries like the benchmark structure "benchy" were fabricated. Furthermore, feature sizes below 100 µm and resolutions of 75–90 µm highlight their suitability for high-resolution 3D printing. Detailed analysis of the mechanoresponse confirmed visual reporting of both compressive and tensile stress, additionally a recovery to the original state for the compressed material was demonstrated. Importantly, presented systems rely on inexpensive commercial monomers and a straightforward synthesis of Sp-dA, making it potentially scalable. We believe that the developed mechanochromic 4D printable materials hold promise for practical applications in failure detection, offering real-time, force-triggered visual signaling.

4. Materials and methods

4.1. Materials

Ethylene glycol dimethacrylate (EGDMA), acrylic acid (AcA), methyl acrylate (MeA), and 1,4-dioxane (dioxane) were bought from Sigma Aldrich GmbH. Ivocerin was provided by Ivoclar Vivadent GMBH. Deuterated solvents were purchased from Deutero GmbH. All other employed chemicals and solvents were purchased from Sigma Aldrich GmbH, Fisher Scientific,

BLDpharm or TCI. All reagents were used without further purification, if not mentioned otherwise.

4.2. Methods

All experiments, except for the tensile test, were performed under yellow light conditions.

4.2.1. Formulation preparation. All the components except for Sp-dA were combined and sonicated for 15 min at room temperature [3400 mg MeA (85.8 wt%), 450 mg EGDMA (11.3 wt%), 40 mg Ivocerin (1.0 wt%),75 mg dioxane (1.9 wt%)] or [4533 mg AcA (96.9 wt%), 112 mg EGDMA (2.0 wt%), 53 mg Ivocerin (1.1 wt%)]. Afterwards, they were combined with Sp-dA (40 mg Sp-dA to the MeA-based formulation; 80 mg SP-dA to the AcA-based formulation) and sonicated for 30 s or shaken for 10 min.

4.2.2. Curing tests. The curing tests were directly performed on the 3D DLP printer. Therefore, a droplet of the AcA-based formulation was applied to a piece of FEP foil (thickness 100 μm) and irradiated in a 2 mm circular spot with a 460 nm wavelength LED (14 mW cm^{-2}). This was repeated for different periods of time. In case of the MeA-based formulation, droplets were added to a PDMS mold on a glass coverslip (Marienfeld, 170 ± 5 μm), before they were irradiated with a circular spot (2 mm diameter) for different periods of time using a 460 nm wavelength LED (14 mW cm^{-2}). Afterwards, for both formulations, the non-polymerized material was washed off with acetone, and the sample was carefully dried with pressurized N_2. The different layer thicknesses of the spots were measured with a caliper. The measured cure depth and corresponding light energy values were plotted semi-logarithmically to obtain the Jacobs working curve.[40]

4.2.3. Digital light processing (DLP). For 3D DLP printing a commercial DLP printer called MONO3Z4 (Microfluidics for all, inc, USA) equipped with a 460 nm wavelength LED (max. intensity = 14 mW cm^{-2}) was used. The digital 3D models were sliced to a layer thickness of 100 μm employing the software MonoWare (Microfluidics for all, inc., USA). The formulations were always freshly prepared before 3D DLP printing. After the print was performed, the 3D structures were rinsed with acetone to remove unpolymerized ink formulation and afterwards carefully dried with pressurized N_2.

4.2.4. Dynamic mechanical analysis (DMA). DMA was performed utilizing a DMA 850 (TA Instruments, USA) device. Bars with dimensions 15 × 3 × 1 mm^3 were printed and used directly for DMA characterization. Measurements were performed using the tension clamp in a temperature range from −70 to 160 °C. A temperature ramp of 3 K min^{-1}, a frequency of 1 Hz, and an amplitude of 0.01% were applied.

4.2.5. Tensile test. The tensile tests were performed with a 2.5kN Zwicki tensile-test device (ZwickRoell GmbH & Co. KG). A 500 N sensor was utilized to perform measurements with a separation speed of 4 mm min^{-1}. As a testing specimen, a nonstandard ''dog bone'' was 3D DLP printed and used for the tensile test without further treatment.

4.2.6. Irradiation experiments. To switch the Sp in the bulk material to the Mc state it was irradiated for 3 min with UV-light in a flash UV chamber (Asiga). The intensity of the UV-light in the Asiga flash chamber was measured at a wavelength of 365 nm with the PM100D from Thorlabs GmbH at 4.83 mW cm^{-2} To switch the Mc back to the Sp, the structures were irradiated with 520 nm wavelength light (71 mW cm^{-2}) for 10 min.

4.2.7. UV/Vis absorption spectroscopy. The UV/Vis absorption measurements were performed with a Jasco V-770 Spectrophotometer (Jasco Deutschland GmbH) device. The UV/Vis experiments in solutions were performed at a concentration of 10^{-4} M Sp-dA in the respective solvent. To ensure that solely the ''closed'' Sp-dA state is present, the cuvette including the Sp-dA containing solution was irradiated with 520 nm wavelength light for 5 min beforehand, to switch all the Mc-dA to Sp-dA. To switch all the Sp-dA to Mc-dA the cuvette was irradiated for 3 min with UV-light. The thin films were produced by adding a droplet of the formulation between two glass cover slides (Marienfeld, 170 ± 5 μm), pressing them together and curing them in the flash UV chamber (Asiga) for 3 min. The film holder FlH-741 was used to measure thin films, and the UCB-710 rectangular cell holder was used to measure dissolved samples in a 1 cm thick quartz glass cuvette.

4.2.8. NMR-spectroscopy. All NMR spectra were recorded on a Bruker Avance III 300 MHz, Bruker Avance III 400 MHz, or Bruker Avance III 500 MHz and processed with MestReNove 14.3.2-32681. Chemical shifts are given in parts per million (ppm) and the shifts for ^1H and ^{13}C NMR spectra were referenced to the locked solvent. The signal patterns are noted as follows: s (singlet), d (doublet), t (triplet), dd (doublet of a doublet), and m (multiplet).

4.2.9. FTIR spectroscopy. A Jasco FT/IR-4600 spectrometer was used to record all FTIR spectra under ambient conditions. All spectra were recorded in a range from 500 to 4000 cm^{-1}.

Author contributions

The manuscript was written through contributions of all authors. All authors have given approval to the final version of the manuscript.

Conflicts of interest

There are no conflicts of interest to declare.

Data availability

Data for this article, including raw data of the characterization of the materials and images are available at HeiData repository at: https://doi.org/10.11588/DATA/ZZBG4O.

Supplementary information (SI) is available. See DOI: https://doi.org/10.1039/d5ma01401h.

Acknowledgements

The authors acknowledge support by German Research Foundation (DFG) within the framework of SFB1249 and the

Excellence Cluster ''3D Matter Made to Order'' (EXC-2082/1-390761711). We also acknowledge the Carl Zeiss Foundation through the ''Carl-Zeiss-Foundation-Focus@HEiKA'', the data storage service SDS@hd supported by the Ministry of Science, Research and the Arts Baden-Württemberg (MWK) and the German Research Foundation (DFG) through grant INST 35/1503-1 FUGG. We also thank the ''Soft (bio)materials characterization'' Core Facility (IMSEAM) at Heidelberg University for their support.

References

1 M. M. Caruso, D. A. Davis, Q. Shen, S. A. Odom, N. R. Sottos, S. R. White and J. S. Moore, *Chem. Rev.*, 2009, **109**, 5755.
2 H. Traeger, D. J. Kiebala, C. Weder and S. Schrettl, *Macromol. Rapid Commun.*, 2021, **42**, 2000573.
3 M. K. Beyer and H. Clausen-Schaumann, *Chem. Rev.*, 2005, **105**, 2921.
4 D. Kim, M. S. Kwon and C. W. Lee, *Polym. Chem.*, 2022, **13**, 5177.
5 J. Ma, Y. Yang, C. Valenzuela, X. Zhang, L. Wang and W. Feng, *Angew. Chem., Int. Ed.*, 2022, **61**, e202116219.
6 G. O'Bryan, B. M. Wong and J. R. McElhanon, *ACS Appl. Mater. Interfaces*, 2010, **2**, 1594.
7 D. A. Davis, A. Hamilton, J. Yang, L. D. Cremar, D. van Gough, S. L. Potisek, M. T. Ong, P. V. Braun, T. J. Martínez, S. R. White, J. S. Moore and N. R. Sottos, *Nature*, 2009, **459**, 68.
8 H. Chen, F. Yang, Q. Chen and J. Zheng, *Adv. Mater.*, 2017, **29**, 1606900.
9 Y. Mao, Y. Kubota, R. Feng, J. Gong, A. Ishigami, Y. Kobayashi, T. Watabe, D. Aoki, H. Otsuka and H. Ito, *Macromolecules*, 2022, **55**, 3948.
10 H. Sakai, D. Aoki, K. Seshimo, K. Mayumi, S. Nishitsuji, T. Kurose, H. Ito and H. Otsuka, *ACS Macro Lett.*, 2020, **9**, 1108.
11 J. R. Hemmer, V. Bauernfeind, C. Rader, M. Petroselli, C. Weder and J. A. Berrocal, *Macromolecules*, 2023, **56**, 8614.
12 J. R. Hemmer, C. Rader, B. D. Wilts, C. Weder and J. A. Berrocal, *J. Am. Chem. Soc.*, 2021, **143**, 18859.
13 K. Ishizuki, H. Oka, D. Aoki, R. Goseki and H. Otsuka, *Chem. – Eur. J.*, 2018, **24**, 3170.
14 K. Imato, A. Irie, T. Kosuge, T. Ohishi, M. Nishihara, A. Takahara and H. Otsuka, *Angew. Chem., Int. Ed.*, 2015, **54**, 6168.
15 K. Imato, M. Nishihara, T. Kanehara, Y. Amamoto, A. Takahara and H. Otsuka, *Angew. Chem., Int. Ed.*, 2012, **51**, 1138.
16 K. Ishizuki, D. Aoki, R. Goseki and H. Otsuka, *ACS Mater. Lett.*, 2018, **7**, 556.
17 M. Li, Q. Zhang and S. Zhu, *Polymer*, 2016, **99**, 521.
18 V. X. Truong, K. Ehrmann, M. Seifermann, P. A. Levkin and C. Barner-Kowollik, *Chem. – Eur. J.*, 2022, **28**, e202104466.
19 S. L. Potisek, D. A. Davis, N. R. Sottos, S. R. White and J. S. Moore, *J. Am. Chem. Soc.*, 2007, **129**, 13808.
20 M. Sommer, *Macromol. Rapid Commun.*, 2021, **42**, 2000597.
21 R. Klajn, *Chem. Soc. Rev.*, 2014, **43**, 148.
22 M. Bayat, H. Mardani, H. Roghani-Mamaqani and R. Hoogenboom, *Chem. Soc. Rev.*, 2024, **53**, 4045.
23 Y. Chen, G. Mellot, D. van Luijk, C. Creton and R. P. Sijbesma, *Chem. Soc. Rev.*, 2021, **50**, 4100.
24 G. I. Peterson, M. B. Larsen, M. A. Ganter, D. W. Storti and A. J. Boydston, *ACS Appl. Mater. Interfaces*, 2015, **7**, 577.
25 X. Meng, G. Qi, X. Li, Z. Wang, K. Wang, B. Zou and Y. Ma, *J. Mater. Chem. C*, 2016, **4**, 7584.
26 C. M. Kingsbury, P. A. May, D. A. Davis, S. R. White, J. S. Moore and N. R. Sottos, *J. Mater. Chem.*, 2011, **21**, 8381.
27 M. Gastaldi, F. Cardano, M. Zanetti, G. Viscardi, C. Barolo, S. Bordiga, S. Magdassi, A. Fin and I. Roppolo, *ACS Mater. Lett.*, 2021, **3**, 1.
28 X. Miao, K. C. H. Chin and A. J. Boydston, *Addit. Manuf.*, 2024, **81**, 104014.
29 A. Basu, J. Wong, B. Cao, N. Boechler, A. J. Boydston and A. Nelson, *ACS Appl. Mater. Interfaces*, 2021, **13**, 19263.
30 A. Bagheri and J. Jin, *ACS Appl. Polym. Mater.*, 2019, **1**, 593.
31 S. C. Ligon, R. Liska, J. Stampfl, M. Gurr and R. Mülhaupt, *Chem. Rev.*, 2017, **117**, 10212.
32 T. Zhang, G. Pacella, K. Chen, T. Ye, G. Portale, V. S. D. Voet, R. Folkersma and K. Loos, *Macromolecules*, 2025, **58**, 8249.
33 E. Takács and L. Wojnárovits, *Radiat. Phys. Chem.*, 1995, **46**, 1007.
34 C. Li, A. Iscen, L. C. Palmer, G. C. Schatz and S. I. Stupp, *J. Am. Chem. Soc.*, 2020, **142**, 8447.
35 Y. Bao, *Macromol. Rapid Commun.*, 2022, **43**, 2200202.
36 N. Moszner, F. Zeuner, I. Lamparth and U. K. Fischer, *Macromol. Mater. Eng.*, 2009, **294**, 877.
37 F. Kröger, L. Schulte, C. A. Spiegel, C. Vazquez-Martel and E. Blasco, *Smart Mater. Struct.*, 2024, **34**, 25001.
38 J. J. Schwartz, R. Behrou, B. Cao, M. Bassford, A. Mendible, C. Shaeffer, A. J. Boydston and N. Boechler, *Polym. Chem.*, 2020, **11**, 1122.
39 M. Li, Q. Zhang, Y.-N. Zhou and S. Zhu, *Prog. Polym. Sci.*, 2018, **79**, 26.
40 P. F. Jacobs, *Rapid Prototyping & Manufacturing: Fundamentals of Stereolithography, Society of Manufacturing Engineering*, Dearborn, MI, 1992.